

Integration of Remote Sensing Data in Rain-on-Grid Flood Modelling and Post-Event Validation Using Orthophotos

Mustafa Berkay Akpinar¹, Zuhal Akyürek^{2,3}

¹ HidroSAF Ltd., Middle East Technical University (METU) Technopolis, Türkiye - berkay.akpinar@hidrosaf.com

² METU, Faculty of Engineering, Dept. of Civil Engineering, Türkiye - zakyurek@metu.edu.tr

³ METU, Graduate School of Natural and Applied Sciences, Dept. of Geodetic and Geographic Information Technologies, Türkiye

Keywords: Rain-on-modelling, Hydrodynamic Simulation of Basins, HEC-RAS 2D, Spatial Validation, Flood Simulation

Abstract

This study explores the integration of remote sensing data into rain-on-grid flood modelling, with a focus on post-event validation using high-resolution orthophotos. The aim is to assess the hydrologic and hydraulic characteristics of the flood event that occurred on August 11, 2021, in Ezine Creek, which flows through the Bozkurt district center located in the north of Kastamonu, Turkey. By comparing the simulated flood extent with observed flood boundaries extracted from orthophotos, the hydraulic model was calibrated to better represent the actual flood behaviour. The resulting hydrograph was then used in the downstream section, where hydraulic structures and debris that contributed to the flooding were explicitly modelled and compared against observed outcomes. This calibration process enabled the derivation of a realistic hydrograph for downstream boundary conditions in subsequent flood event simulations. The approach demonstrates the value of combining remote sensing and traditional hydraulic modelling for enhanced flood risk assessment and decision-making.

1. Introduction

Satellite images play a crucial role in flood modelling, offering valuable data before, during, and after flood events. Their use enhances the accuracy, timeliness, and spatial coverage of flood assessments. Flood modelling using hydrodynamic simulation tools is essential for understanding and mitigating disaster impacts, particularly in ungauged or data-scarce regions (Zeiger and Hubbart, 2021). With recent developments in remote sensing technologies and hydraulic modelling platforms, rainfall-runoff processes can now be simulated with higher spatial and temporal resolutions with full momentum equations (Enea et al., 2018). Since the uncertainties are inevitable in flood modelling, models must be validated with all possible available data depending on the utilized model (Bates et al., 2021). This study presents a rain-on-grid flood modelling approach for Bozkurt Flood Event in 2021 using HEC-RAS 2D, where open-source remote sensing datasets were integrated for land use and soil group characterization and the estimation of essential hydrographs. The simulated flood extents were validated using high-resolution post-event orthophotos (Clasing et al., 2023). The use of open-source spatial data and orthophotos has increased the accuracy of the model results.

2. Materials and Methods

2.1 Study Area and Data

Bozkurt is located in the north of Kastamonu province, along the Black Sea coast (Figure 1). The town centre is situated 2 km inland in the valley of the Ezine Stream. It is bordered by the Black Sea and Abana to the north, Küre and Devrekani to the south, Çatalzeytin to the east, and Abana to the west. The district has a surface area of 296 km² and an elevation of 30 meters. The coastline stretching along the Black Sea is approximately 10.5 km long.

The Ezine Stream (also known as Büyük Çay) originates in the Devrekani district, passes through the lands of Küre, and enters the borders of Bozkurt. From there, it receives the Keşlik and Maraz streams, then splits the district into two through the

Sinarcık and Yılmaz neighborhoods and the Pazaryeri area, and finally discharges into the sea at a place called Harmoson in Abana whose length is 60 km. The İlişi Stream originates from the Küre district and passes through Bozkurt, flowing into the sea from the village of İlişi (Yakaören). Its length is approximately 40 km. Since the Ezine and İlişi streams have irregular flow patterns, they cause flood events during heavy rainfall.

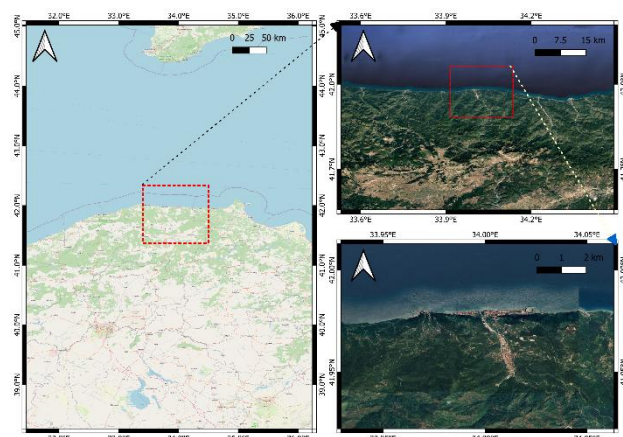


Figure 1. Location of the study area.

When the basin and its hypsometric curve are analysed, it is observed that the upper and lower parts of the basin exhibit very steep drops in elevation, indicating rapid surface runoff, higher erosion potential, short concentration times, and high flow velocities. The middle part of the basin (20–80%) represents a gentler slope and acts as a transition zone where the flow slows down, allowing for more balanced sediment transport (Figure 2).

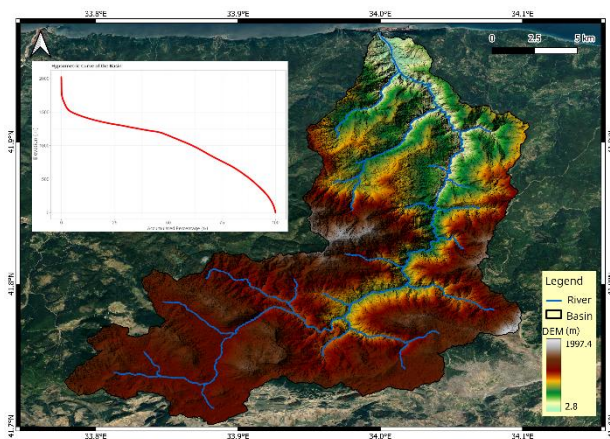


Figure 2. DEM and hypsometric curve of the study area.

For land cover information, the ESA WorldCover product (ESA CCI, 2017) with a 10-meter resolution was used. This dataset, derived from Sentinel-1 and Sentinel-2 data, provides detailed land cover classifications at high spatial resolution (Figure 3). It distinguishes between land cover types such as trees, shrublands, grasslands, croplands, built-up areas, barren or sparse vegetation, snow and ice, open water, herbaceous wetlands, mangroves, and mosses and lichens. Analysis of the watershed indicates that tree cover is the dominant land cover type in the region. Tree cover is particularly sensitive in flood modelling due to its influence on surface roughness, which is affected by structural density parameters such as trunk count, underbrush, and canopy cover. It is also one of the most challenging land cover types for assigning an appropriate Manning's roughness coefficient (Arcement & Schneider, 1989). Depending on its density, the Manning's n value for tree cover may range from 0.07 to 0.4.

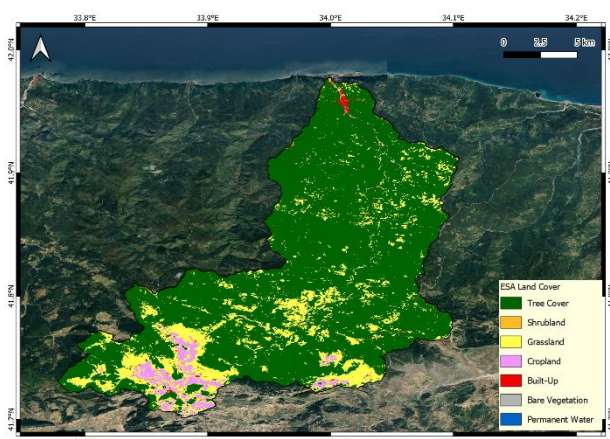


Figure 3. ESA Land Cover of the study area.

The flood event that occurred on August 10–11, 2021, in the western Black Sea region was selected for this study. According to observations from meteorological stations within the 372.5 km² basin, the rainfall recorded on August 11, 2021, in Bozkurt/Mamatlar was 394 mm, significantly higher than the maximum rainfall recorded in 2017, which was 73 mm (Table 1).

The peak discharge resulting from this storm exceeded the design discharge of the Ezine River cross-section, which passes through Bozkurt. The study area was modeled using HEC-RAS with the Rain-on-Grid approach. This method may require different input

parameters depending on the infiltration method chosen by the modeler. In this study, the SCS Curve Number method was used.

Station	Date	Max. Precip	Date	Max. Precip
Kastamonu	3.5.1953	104.7	11.08.2021	298.8
Bartın	27.08.1970	161.1	11.08.2021	302.4
Sinop	19.04.1948	203.2	11.08.2021	240.5
Bozkurt	1988	143.0	11.08.2021	120
Devrekani	1999	55.6	11.08.2021	132.6
Bozkurt/Mamatlar	2017	72.7	11.08.2021	294.1

Table 1. Precipitation amounts on the event day and maximum rainfall magnitudes observed earlier.

Meteorological stations named as Küre, Devrekani, Mamatlar, and Bozkurt were used to generate a spatial precipitation grid, preserving both peak rainfall amounts and temporal variability. To implement the 2D shallow water equations (HEC-RAS User's Manual, 2023), surface roughness values were calculated using the ESA 2021 Land Cover dataset, as previously described. Hydrological Soil Groups (HSGs) were obtained from the open-access 'HYSOGs250m' dataset, which provides eight distinct soil groups for both drained and undrained conditions (Ross et al., 2018). A Digital Elevation Model (DEM) with a 5-meter spatial resolution was used for hydrodynamic modeling of the entire watershed. Since the flood extent was identified using post-event orthophotos (Figure 4) and the timing of peak flows was verified through local camera footage, the model was calibrated accordingly to capture flow accumulation across the 372.5 km² watershed. Following validation, the relevant hydrograph that reached the downstream main channel and caused the overflow was determined.

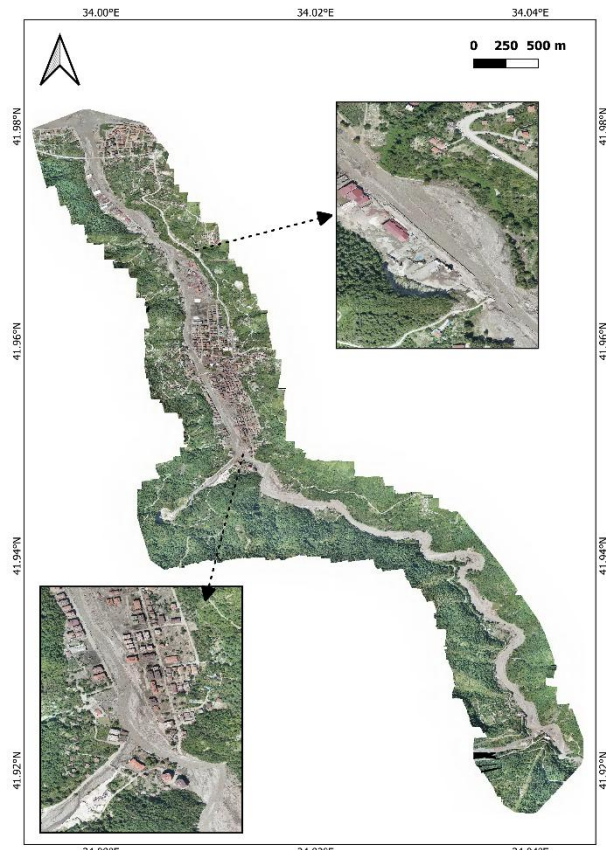


Figure 4. Orthophoto of the downstream parts of the study area.

2.2 Hydraulic Modelling

Two hydraulic models were developed for this study. The first model was created for the previously mentioned overall watershed using a Digital Elevation Model (DEM) with a 5-meter resolution. The Rain-on-Grid approach was applied in this model, using the SCS Curve Number infiltration method. Rain-on-Grid modelling in HEC-RAS is a 2D hydrologic-hydraulic approach in which rainfall is applied directly to each cell of the terrain grid (HEC-RAS User's Manual, 2023) (Figure 5). The model calculates runoff generation and surface flow based on rainfall intensity, land characteristics, and topography. It employs infiltration methods such as the SCS Curve Number, Green-Ampt, or constant loss to estimate the portion of rainfall that becomes runoff. The resulting runoff is then routed across the terrain using slope and surface roughness values (Manning's n). Hydraulic structures such as culverts, bridges, and weirs can be incorporated to simulate real-world conditions. This method is particularly useful for modelling urban flooding, flash floods, or natural terrain responses without the need for external inflow hydrographs. Rain-on-Grid modelling provides a more physically based simulation but requires high-quality rainfall and topographic data. It is also more computationally intensive than traditional methods such as HEC-HMS. According to the literature, the Rain-on-Grid approach has proven to be highly useful for flood risk management (Clasing et al., 2023), and very realistic results can be achieved through a proper calibration process (Costabile et al., 2021).

The spatial distribution of the rainfall was obtained using the observations at the meteorological stations and the interpolated total precipitation for the basin for the storm occurred on August 11, 2021 is given in Figure 6.

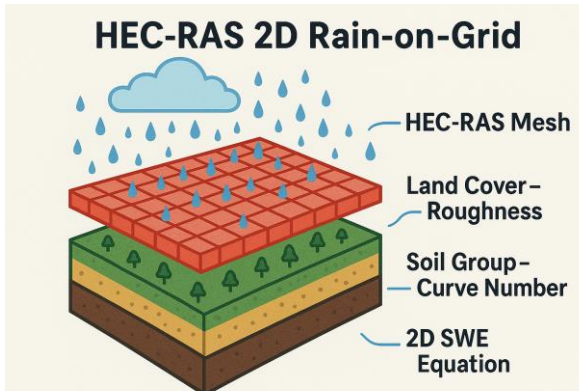


Figure 5. Rain-on-grid approach for basin hydrodynamics

Another model was developed for the downstream sections, which required more detailed analysis and accurate representation of hydraulic structures, using a 1-meter resolution DEM. The hydrograph obtained from the overall watershed model was used as input for this model to simulate the actual flood event and overtopping conditions. HEC-RAS was again employed, this time using the full momentum equations with conservative turbulence modelling to account for complex hydraulic behaviour, such as bridge overtopping, debris blockages, and sudden velocity changes—particularly around residential areas.

Bathymetric data, surrounding buildings and the existing bridges were also incorporated into the model to realistically capture all

hydraulic behaviours (Figure 7), where mentioned obtain hydrograph was also observed.

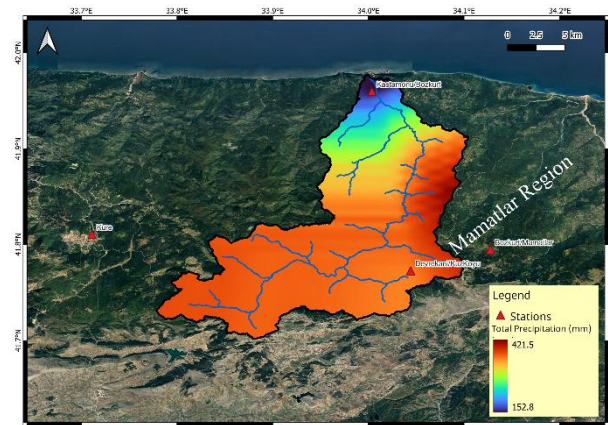


Figure 6. Interpolated total precipitation from different stations.

During the peak flow of the event, debris blockages led to the collapse of several bridges, particularly the main vehicle bridge, where the primary overflow and resulting floodplain flow originated (Figure 8). For this reason, debris blockages of 1 meter and 1.5 meters were modelled to observe their effects on overflow behaviour and overall hydraulic response.



Figure 7. Modelled bridges.



Figure 8. Debris blockage of main vehicle bridge.

3. Results and Discussions

Since the entire flood event was recorded by locals using cameras, and the flood extent was captured by aerial imagery shortly afterward, the overall watershed hydraulic model was calibrated both temporally and spatially.

The gridded distribution methods of precipitation and the selection of Manning's roughness coefficients are critical parameters for realistically simulating flood propagation. HEC-RAS allows modelers to interpolate station-based precipitation data using four different methods: Thiessen Polygons, Inverse Square of Distance, Inverse Distance Restricted, and Peak Preservation. For this event, the Peak Preservation technique was found to be the most appropriate, as rainfall accumulation, particularly from channels originating in Mamatlar (location is presented in Figure 6), led to a sudden increase in hydrograph values.

Another important aspect of the calibration process was the use of recorded images and videos to determine the timing of the flood event and, specifically, the peak flow period in overtopped regions. The visual data revealed two distinct hydrograph peaks (Figure 9). The location of the x-section where the hydrograph is obtained is presented in Figure 7. The first peak, which occurred around noon on the first day, passed through the channel without causing overflow, utilizing approximately 55–65% of its total capacity. The second peak, reaching approximately 1200 m³/s, began to overflow, particularly after debris blockage, at around 13:00 on August 11. The regulated cross-section of the Ezine Stream has been designed based on a 500-year return period flow (Q500 = 522 m³/s) and includes a 30 cm freeboard.

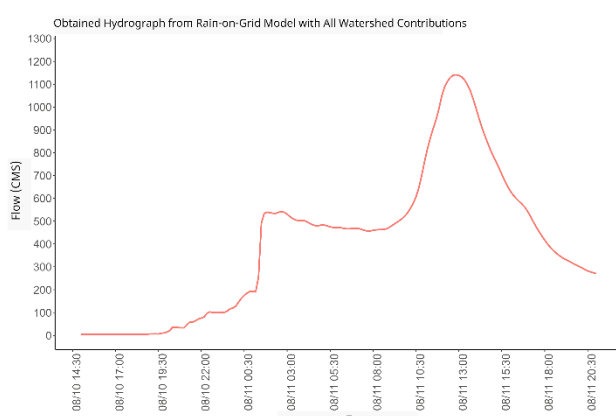


Figure 9. Hydrograph obtained for the storm event.

The calibrated model, using orthophotos captured shortly after the flood event, accurately represents the flood extent (Figure 10). This extent was instrumental in calibrating the roughness parameters and selecting appropriate gridded precipitation interpolation techniques. The timing of flood event was checked from the recorded images (Figure 11).

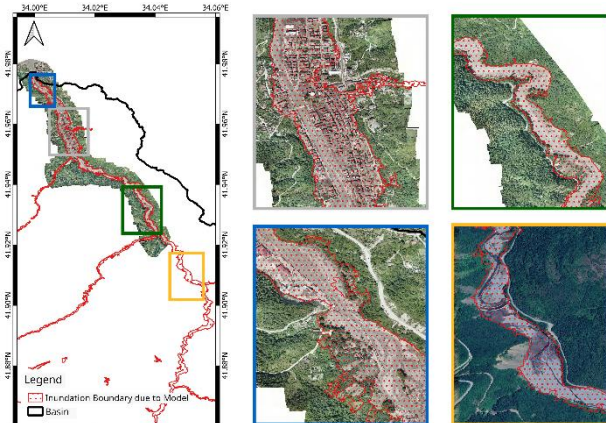


Figure 10. Inundation boundary of the model calibrated with orthophoto.



Figure 11. Timing of flood event with recorded images.

The second peak flow (≈ 1200 m³/s), as previously mentioned, began to overflow from the right bank of the critical bridge due to debris blockages. Shortly afterward, all affected bridges collapsed. The bridge overflow was modelled and the streamlines obtained from the model indicate the high-water velocity from the right of the bridge x-section (Figure 12). The hydraulic jump occurred at the downstream of the collapsed bridge is modelled as well.

The atmospheric and surface conditions that caused the flood disaster constitute a catastrophic event (the highest value that can be observed during the observation period) resulting in extremely intense rainfall. When examining the rainfall values observed during the event, it is clear that they even exceed the estimates made for a 1000-year daily event. Moreover, the 2-hour rainfall amount (around 100 mm) is also seen to be greater than the 1000-year rainfall magnitude.



Figure 12. Bridge overflow and its model in HEC-RAS

4. Conclusions

This study explores the integration of remote sensing data into Rain-on-Grid flood modelling, with a particular focus on post-event validation using high-resolution orthophotos of a real flood event that occurred on August 11, 2021, in Ezine Creek, which flows through the Bozkurt district centre in northern Kastamonu, Turkey. Since the stream gauge was damaged and lost during the event, all available sources were investigated to determine and analyse the hydrological and resulting hydraulic parameters of this devastating flood.

Although modelling tools are now widely accessible and user-friendly, calibration of these models still remains critically important. Uncertainties in input parameters (e.g., hyetographs, hydrographs, roughness coefficients, and soil/land cover characteristics) can lead to under- or overestimation of actual outputs, both spatially and temporally (Apel et al., 2008), (Akpinar, 2023).

A Rain-on-Grid model of the entire watershed was developed to obtain the hydrological and hydraulic outputs of the flood event. Gridded precipitation data were used based on the availability of measurements from four meteorological stations. Accurate flood timing data and orthophotos captured shortly after the event were used to calibrate the Manning's roughness coefficients, initial abstractions, and the interpolation method for the precipitation grid.

Results indicate that the flood event was simulated with a high degree of realism, both temporally and spatially. The first peak of the hydrograph passed through the channel without causing overflow. The second peak, approximately 1200 m³/s, combined with 1-meter debris blockages, resulted in overflow timings consistent with observed bridge overtopping.

References

Akpinar, M. B. (2023). A Study on Uncertainty-Based Flood Analysis (Master's thesis, Middle East Technical University (Turkey)).

Apel, H., Merz, B., & Thielen, A. H. (2008). Quantification of uncertainties in flood risk assessments. International Journal of River Basin Management, 6(2), 149-162.

Arcement, G. J., Jr., & Schneider, V. R. (1989). Guide for selecting Manning's roughness coefficients for natural channels and flood plains (Water-Supply Paper No. 2339). U.S. Geological Survey

Bates, P., Neal, J., Sampson, C., Smith, A., 2021. Flood inundation modeling: A review of methods and applications. WIREs Water, 8(2), e1501. <https://doi.org/10.1002/wat2.1501>

Chaitanya, J. C., Sridharan, B., & Kuiry, S. N. (2024). The rain-on-grid modeling approach in hydrological and hydraulic processes over a river basin. In World Environmental and Water Resources Congress 2024 (pp. 221-232).

Clasing, J., Müller, R., Tschada, H., 2023. Remote sensing with UAVs for flood modeling: A validation with actual flood records. Int. Arch. Photogramm. Remote Sens. Spatial Inf. Sci., XLVIII-3/W1-2023, 241–248. <https://doi.org/10.5194/isprs-archives-XLVIII-3-W1-2023-241-2023>

Costabile, P., Costanzo, C., Ferraro, D., & Barca, P. (2021). Is HEC-RAS 2D accurate enough for storm-event hazard assessment? Lessons learnt from a benchmarking study based on rain-on-grid modelling. Journal of Hydrology, 603, 126962.

Enea, M., Mihalache, S., Neagu, C., 2018. Flood extent validation using Landsat, LiDAR, and HEC-RAS. Int. Arch. Photogramm. Remote Sens. Spatial Inf. Sci., XLII-2/W7, 29–36. <https://doi.org/10.5194/isprs-archives-XLII-2-W7-29-2018>

ESA CCI, 2017. European Space Agency Climate Change Initiative – Land Cover Product 2015. Land Cover CCI Product User Guide Version 2.0. <https://www.esa-landcover-cci.org>

HEC-RAS User's Manual, 2023. HEC-RAS 2D Rain-on-Grid Modeling. Version 6.4. U.S. Army Corps of Engineers, Hydrologic Engineering Center. <https://www.hec.usace.army.mil/software/hec-ras/documentation/>

Ross, C. W., Prihodko, L., Hanan, N. P., Anchang, J., 2018. HYSGOs250m: Global gridded hydrologic soil groups for curve-number-based runoff modeling. Earth Syst. Sci. Data, 10, 1237–1243. <https://doi.org/10.5194/essd-10-1237-2018>

Zeiger, S. J., Hubbart, J. A., 2021. Integrated modeling of flood events using SWAT and HEC-RAS 2D. Water, 13(17), 2346. <https://doi.org/10.3390/w13172346>